Asymptotic analysis of the attractors in two-dimensional Kolmogorov flow

W. R. SMITH [1], and J. G. WISSINK [2]

[1] *School of Mathematics, The University of Birmingham, Edgbaston, Birmingham, B15 2TT, UK.*
email: W.Smith@bham.ac.uk
[2] *Department of Mechanical, Aerospace and Civil Engineering, Brunel University, Uxbridge, Middlesex, UB8 3PH, UK.*

(*Received 14 March 2017*)

The high-Reynolds-number structure of the laminar, chaotic and turbulent attractors is investigated in a two-dimensional Kolmogorov flow. The laminar attractors include the families of multi-phased travelling waves and quasi-periodic standing waves both of which form the backbone of the transition to a turbulent flow. At leading order, each laminar attractor under study is obtained by solving the Euler equations on a manifold subject to the appropriate periodicity and symmetry conditions. The manifold is determined by a finite number of vorticity equations, these being required to suppress the secular terms at the next order. Our results show that, for the multi-phased travelling waves, the first phase velocity can be determined by an integral conservation law for kinetic energy and the subsequent phase velocities can be evaluated by a nonlinear eigenvalue problem. The results also reveal that whereas viscosity determines the smallest scales and controls the amplitude of the flow, the inertial terms govern the shape and form of the flow. The comparison of our analytical predictions for evaluating the stable single-phased travelling wave with the direct numerical simulation of the Navier–Stokes equations has been undertaken, the agreement being excellent. For sufficiently high Reynolds number, after the bifurcation to chaotic flow, all of the multi-phased travelling waves and quasi-periodic standing waves become unstable non-wandering sets. Based on the above new findings for these unstable non-wandering sets and other travelling and standing waves of this kind in phase space, necessary conditions for the invariant manifolds of the chaotic and turbulent attractors are obtained, these necessary conditions being conjectured to be also sufficient.

Key Words: singular perturbations, waves, Navier–Stokes equations

1 Introduction

Free-space high-Reynolds-number laminar flow has not been extensively studied using perturbation theory despite having long been viewed as a missing ingredient in the understanding of the elementary interaction of vortices and the development of statistical models for turbulent flow [3]. The extent of the use of asymptotic analysis in this case may be contrasted with the study of wall-bounded shear flows at high Reynolds number, with the latter having achieved significant success in the application of boundary-layer theory over many decades. The most prominent examples include uniform flow over a semi-infinite plate [30, 31], Hagen-Poiseuille flow [29] or vortex-wave interaction theory [11], the nonlinear analytical predictions in [29] having been confirmed numerically in [9]. More recently, asymptotic analysis has also succeeded in predicting the shrinkage of the domain of attraction of the basic flow for both plane Couette flow and plane Poiseuille flow [7].

For many decades, leading scientists have articulated the importance of the study of the Navier–Stokes equations using viable formal perturbation schemes [3, 8, 40]. In 1948, Hopf made conjectures regarding the attractors of the Navier–Stokes equations; in particular, their response to an increase in Reynolds number and their relationship with turbulent flow. Alas, he eventually concluded that [13] "the way to a successful attack on them seems hopelessly barred." A decade later, in Kolmogorov's 1958 seminar on dynamical systems and hydrodynamic stability, eight open problems were introduced. It is Kolmogorov's fifth open problem that guides us in this article towards a successful strategy of attack on the analysis of the attractors, namely [3] "the mathematical theory of partial differential equations containing a small parameter multiplying the term with the highest derivative; until now only such phenomena as boundary layers or interior layers have been studied." Fortunately, the most recent progress on Kolmogorov's fifth open problem presents us with an opportunity to address Hopf's open problems on the attractors of the Navier–Stokes equations in a simple free-space high-Reynolds-number flow.

In the context of transition to turbulence, the attractors of the Navier–Stokes equations were first studied by Landau [18] and Hopf [13] who envisaged a sequence of attractors which were at first periodic with a single frequency and then quasi-periodic with a growing number of fundamental frequencies as the Reynolds number increased. Each attractor originated at one of an infinite sequence of bifurcations. This infinite sequence of attractors was subsequently limited to the Ruelle–Takens scenario, which predicted that a quasi-periodic solution with more than three fundamental frequencies is, in general, unstable [24, 27]. Hopf [13] also conjectured that, owing to the action of viscosity, these attractors resided on a finite-dimensional invariant manifold in phase space. More recently, further evidence has been provided that viscous effects are not entirely confined to small scales; that is, the inviscid dominance on the broader scales needs to be supplemented due to the occurrence of vortex eruptions [6]. These are sporadic events involving unsteady separations and breakups of the local and global flow structure which originate from viscous effects.

While Kolmogorov [3] was the first to anticipate the link between the attractors of the Navier–Stokes equations and high-Reynolds-number asymptotic methods, the firm foundation of this subject was laid by Kuzmak [16] in his study of ordinary differential equations. His analysis facilitated the determination of limit cycles or periodic attractors. Luke [20] extended the methods of Kuzmak to partial differential equations which allowed the prediction of the single-phased travelling wave. Luke's analysis was itself extended to multi-phased travelling waves by Ablowitz and Benney [1]. Meanwhile, equivalent results were derived by Whitham using the averaged Lagrangian principle [41]. Out of all possible approaches, it is the method of Kuzmak–Luke which we choose for investigating the attractors of the Navier–Stokes equations in this article (see the discussion in [39]).

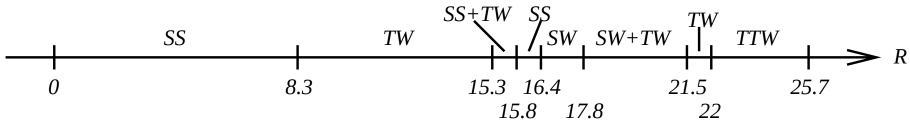

Figure 1. A symbolic diagram specifying the laminar attractors of Kolmogorov flow for aspect ratio $k = 1$, forcing wavenumber $K = 2$ and Reynolds number in the range $0 \leqslant R < 25.7$ (see [2] and Section 2 for the definition of Reynolds number R): stable steady states are denoted by SS; stable single-phased travelling waves by TW; stable periodic standing waves by SW, stable two-phased travelling waves by TTW and bistability of two types of attractor by $+$. The flow becomes chaotic for Reynolds number greater than 25.7.

The method of Kuzmak–Luke has recently been successful in describing single-phased travelling waves on the upper-energy solution branch in two-dimensional plane Poiseuille flow [39]. The presence of viscous boundary layers added complexity to this demanding problem; namely, the Fredholm alternative could not be applied. Even after the necessary modulation equations had been determined, it was impossible to demonstrate their sufficiency. Despite the mathematical difficulty faced in our earlier study, we have found a way to discover the high-Reynolds-number asymptotic structure. Essentially, the attractor is obtained by solving the Euler equations on a manifold subject to periodicity and symmetry conditions. This structure does not apply to the two-phased travelling wave due to the injection of vortex sheets from the walls into the body of the flow. In other words, the method of Kuzmak–Luke turns out to be invalid for all flows involving separation into the inviscid bulk. Therefore, transition to turbulence could not be investigated in the context of two-dimensional plane Poiseuille flow.

In order to gain physical understanding of the transition from laminar to turbulent flows, Kolmogorov also proposed a simplified hydrodynamic model: an incompressible viscous fluid on a torus under the action of a prescribed forcing [4]. It is usually taken to be two-dimensional with harmonic forcing. This Kolmogorov flow is more tractable than other simplified models because it has no walls. There are three main advantages associated with periodic boundary conditions. Firstly, whole families of laminar attractors in the transition to turbulence are amenable to asymptotic methods. Secondly, the absence of viscous boundary layers allows the application of the Fredholm alternative which simplifies our analysis of the manifold. Thirdly, the bifurcations occur at much lower Reynolds number in comparison to wall-bounded shear flows, which produces the significant advantage of substantially reducing the dimension of phase space. Finally, we note that interior viscous layers have been observed at very large Reynolds number [15, 25]. Henceforth, it is assumed that there are no interior viscous layers in the cases studied herein.

Two-dimensional Kolmogorov flow has been widely studied in terms of varying the aspect ratio of the domain [25] and different choices of forcing wavelength [2, 26, 28]. More recent studies are dominated by numerical computations and the dynamical systems point of view [10, 12, 15, 19]. While our asymptotic analysis is applicable to a range of aspect ratios, forcing wavelengths and Reynolds numbers, the examples provided in this article focus on two-dimensional Kolmogorov flow with the particular choice of aspect ratio and

Table 1. Summary of the symmetries of non-wandering sets in two-dimensional plane Poiseuille flow and two-dimensional Kolmogorov flow for aspect ratio $k = 1$ and forcing wavenumber $K = 2$ (see [2] and Section 2 for the definition of Reynolds number R).

	single-phased travelling wave	two-phased travelling wave	periodic standing wave
plane Poiseuille flow	shift-and-reflect symmetry	shift-and-reflect symmetry in the second phase	not applicable
Kolmogorov flow	shift-and-reflect symmetry	shift-and-reflect symmetry in the second phase	shift-and-rotate symmetry for Reynolds number $16.4 < R < 17.0$

forcing wavenumber in [2]. Figure 1 summarizes the laminar attractors for a range of Reynolds number. The single-phased and two-phased stable travelling waves are denoted by TW and TTW, respectively. We note that there are no stable travelling waves with three phases in Figure 1. Furthermore, there are two families of periodic standing waves separated by a nonlocal bifurcation and no stable standing waves with two (or three) fundamental frequencies have been reported for this aspect ratio and forcing wavelength. The stable periodic travelling waves are denoted by SW in Figure 1.

In order to find the appropriate solution, it is necessary that we incorporate any invariance of non-wandering sets under the relevant symmetry groups. In our earlier study of two-dimensional plane Poiseuille flow [39], the shift-and-reflect symmetry provided an additional condition for the single-phased travelling wave. Furthermore, our numerical simulations indicated that the two-phased travelling wave in plane Poiseuille flow does demonstrate a shift-and-reflect symmetry even though it is observed only in the new phase which was acquired at the supercritical Hopf bifurcation. In the current study of Kolmogorov flow, we benefit from the fact that the symmetry structure has been comprehensively identified in [2], the structure for the single-phased and two-phased travelling waves being the same as in the two-dimensional plane Poiseuille flow (see Table 1). In all of these cases, symmetry also offers the significant advantage of reducing the dimension of phase space.

The purpose of this article is to address Hopf's conjecture by investigating the different manifolds associated with laminar, chaotic and turbulent attractors. Of these, the invariant manifold of the turbulent attractor is of greatest interest. Since it is not possible to apply asymptotic analysis directly to the turbulent attractor - an indirect approach has been adopted. Our indirect approach is based on gaining as much insight as possible into the high-Reynolds-number structure of the laminar attractors involved in the transition to turbulence. Accordingly, we investigate the families of both multi-phased travelling waves and quasi-periodic standing waves for Kolmogorov flow, manifolds being sought for each case.

Section 2 describes the mathematical model for two-dimensional Kolmogorov flow which will be studied herein. The asymptotic analysis of the family of multi-phased travelling waves is undertaken in Section 3, the manifold being determined by solvability conditions. Section 4 briefly summarizes the analysis of the manifold for the family of quasi-periodic standing waves, the analysis being similar to the previous section. Sections 5 and 6 utilize the results from Section 3 to expand the description of the asymptotic solution of single-phased and two-phased travelling waves, respectively. Section 5 also presents a comparison of the analytical predictions for the single-phased travelling wave with the results of direct numerical simulation of the Navier–Stokes equations. In Section 7, based on the newly acquired results for these unstable non-wandering sets in Sections 3 and 4, necessary conditions for the invariant manifolds of the chaotic and turbulent attractors are obtained. Finally, Section 8 gives a brief discussion of the results.

2 Mathematical model

In this section, the initial boundary value problem for an incompressible viscous fluid on a two-dimensional torus under the action of harmonic forcing is introduced and scaled. We define ρ to be the density, ν the kinematic viscosity and G a constant pressure gradient. The two-dimensional Navier–Stokes and continuity equations are

$$\frac{\partial \boldsymbol{q}^*}{\partial t^*} + (\boldsymbol{q}^* \cdot \boldsymbol{\nabla}^*)\boldsymbol{q}^* + \frac{1}{\rho}\boldsymbol{\nabla}^* p^* = \nu \Delta^* \boldsymbol{q}^* + \frac{G}{\rho}\boldsymbol{f}$$

and

$$\boldsymbol{\nabla}^* \cdot \boldsymbol{q}^* = 0,$$

respectively, in which $(x^*, y^*)^T$ are the spatial coordinates, t^* is time, $\boldsymbol{q}^* = (u^*, v^*)^T$ are the fluid velocities, p^* is pressure, $G\boldsymbol{f}/\rho$ is the body force and $\boldsymbol{f} = (f, 0)^T$. The periodic boundary conditions are

$$\boldsymbol{q}^*(0, y^*, t^*) = \boldsymbol{q}^*(L^*/k, y^*, t^*), \qquad \boldsymbol{q}^*(x^*, 0, t^*) = \boldsymbol{q}^*(x^*, L^*, t^*),$$

where L^* is the domain width and k is the aspect ratio. We transform to dimensionless variables via

$$x^* = \frac{L^* x}{2\pi}, \qquad y^* = \frac{L^* y}{2\pi}, \qquad t^* = \frac{L^* t}{2\pi U^*}, \qquad u^* = U^* u, \qquad v^* = U^* v, \qquad p^* = \rho {U^*}^2 p,$$

where $U^* = G L^{*2}/(2\pi)^2 \rho\nu$. The governing equations become

$$\frac{\partial \boldsymbol{q}}{\partial t} + (\boldsymbol{q} \cdot \boldsymbol{\nabla})\boldsymbol{q} + \boldsymbol{\nabla} p = \epsilon\, [\Delta \boldsymbol{q} + \boldsymbol{f}] \tag{2.1}$$

and

$$\boldsymbol{\nabla} \cdot \boldsymbol{q} = 0, \tag{2.2}$$

in which ϵ is the reciprocal of the Reynolds number R given by

$$0 < \epsilon = \frac{1}{R} = \frac{2\pi\nu}{U^* L^*} \ll 1$$

and $\boldsymbol{q}$ is the velocity vector $(u, v)^T$. The periodic boundary conditions become

$$\boldsymbol{q}(0, y, t) = \boldsymbol{q}(2\pi/k, y, t), \qquad \boldsymbol{q}(x, 0, t) = \boldsymbol{q}(x, 2\pi, t). \tag{2.3}$$

The kinetic energy is defined by $E = \boldsymbol{q} \cdot \boldsymbol{q}/2$ and the vorticity by $\omega = \partial v/\partial x - \partial u/\partial y$. We consider Kolmogorov flow with the monochromatic forcing $f(y) = K^3 \cos(Ky)$, where K is the forcing wavenumber.

Basic Kolmogorov flow $\boldsymbol{q} = (K\cos(Ky), 0)^T$ and $p =$ constant is an exact solution of the governing equations. The linear stability of this steady state has been investigated analytically [21]. (For $k = 1$ and $K = 2$ in Figure 1, this steady state is stable for $0 \leqslant R < 2$.) The flow typically undergoes a number of bifurcations as the Reynolds number is increased [2, 26, 28], the attractors in the form of multi-phased travelling waves being the main topic of our analysis. We note that our analysis will not be valid for long domains ($k \ll 1$) or for large forcing wavenumber ($K \gg 1$).

3 Multi-phased travelling wave

The following analysis applies to the whole family of multi-phased travelling waves. Each member of this family has a different shift-and-reflect symmetry condition and a different definition of the stream function. Therefore, these details, which are specific to a family member, are postponed until Sections 5 and 6.

3.1 The leading-order problem

The inviscid leading-order problem is considered and it is assumed that there are no interior layers. We adopt N fast phases $\theta_{(j)}$ defined by $\partial\theta_{(j)}/\partial x = k$ and $\partial\theta_{(j)}/\partial t = -\sigma_{(j)}$, where $\sigma_{(j)}$ is a constant frequency and $N \in \{1, 2, 3\}$. The limitation to a maximum of three phases follows from the Ruelle–Takens scenario [24, 27]. (The possibility of $N > 3$ will be discussed in Section 7.) Expansions are introduced of the form

$$\begin{aligned}
u &\sim u_0(\theta_{(1)}, \theta_{(2)}, \ldots, \theta_{(N)}, y) + \epsilon u_1(\theta_{(1)}, \theta_{(2)}, \ldots, \theta_{(N)}, y),\\
v &\sim v_0(\theta_{(1)}, \theta_{(2)}, \ldots, \theta_{(N)}, y) + \epsilon v_1(\theta_{(1)}, \theta_{(2)}, \ldots, \theta_{(N)}, y),\\
p &\sim p_0(\theta_{(1)}, \theta_{(2)}, \ldots, \theta_{(N)}, y) + \epsilon p_1(\theta_{(1)}, \theta_{(2)}, \ldots, \theta_{(N)}, y),\\
E &\sim E_0(\theta_{(1)}, \theta_{(2)}, \ldots, \theta_{(N)}, y) + \epsilon E_1(\theta_{(1)}, \theta_{(2)}, \ldots, \theta_{(N)}, y),\\
\omega &\sim \omega_0(\theta_{(1)}, \theta_{(2)}, \ldots, \theta_{(N)}, y) + \epsilon \omega_1(\theta_{(1)}, \theta_{(2)}, \ldots, \theta_{(N)}, y),
\end{aligned}$$

as $\epsilon \to 0$. At leading order, we obtain

$$\bar{L}u_0 + \sum_{j=1}^{N} k \frac{\partial p_0}{\partial \theta_{(j)}} = 0, \tag{3.1 a}$$

$$\bar{L}v_0 + \frac{\partial p_0}{\partial y} = 0, \tag{3.1 b}$$

$$\sum_{j=1}^{N} k \frac{\partial u_0}{\partial \theta_{(j)}} + \frac{\partial v_0}{\partial y} = 0, \tag{3.1 c}$$

with the differential operator

$$\bar{L} = \sum_{j=1}^{N} k(u_0 - U_{(j)}) \frac{\partial}{\partial \theta_{(j)}} + v_0 \frac{\partial}{\partial y},$$

periodic boundary conditions

$$\begin{aligned}
[u_0, v_0, p_0](0, \theta_{(2)}, \ldots, \theta_{(N)}, y) &= [u_0, v_0, p_0](2\pi, \theta_{(2)}, \ldots, \theta_{(N)}, y), \\
[u_0, v_0, p_0](\theta_{(1)}, 0, \ldots, \theta_{(N)}, y) &= [u_0, v_0, p_0](\theta_{(1)}, P_{(2)}, \ldots, \theta_{(N)}, y), \\
&\vdots \\
[u_0, v_0, p_0](\theta_{(1)}, \theta_{(2)}, \ldots, 0, y) &= [u_0, v_0, p_0](\theta_{(1)}, \theta_{(2)}, \ldots, P_{(N)}, y), \\
[u_0, v_0, p_0](\theta_{(1)}, \theta_{(2)}, \ldots, \theta_{(N)}, 0) &= [u_0, v_0, p_0](\theta_{(1)}, \theta_{(2)}, \ldots, \theta_{(N)}, 2\pi),
\end{aligned} \tag{3.2}$$

$U_{(j)} = \sigma_{(j)}/k$, $P_{(2)}$ and $P_{(3)}$ are constant periods. Quasi-periodicity requires that $2\pi/\sigma_{(1)}$, $P_{(2)}/\sigma_{(2)}$ and $P_{(3)}/\sigma_{(3)}$ are not rational multiples of each other. We take the curl of (3.1 *a*)-(3.1 *b*) to obtain $\bar{L}\omega_0 = 0$ where the leading-order vorticity ω_0 is given by

$$\omega_0 = \sum_{j=1}^{N} k \frac{\partial v_0}{\partial \theta_{(j)}} - \frac{\partial u_0}{\partial y}.$$

The constant $U_{(1)}$ is determined by an integral conservation law during the transient prior to the formation of the attractor (see [39]); henceforth, knowledge of this constant will be assumed while investigating the equations for the attractors. We note that the phase velocity $U_{(1)}$ is not dependent on the exact structure of the solution which classifies the first phase as a travelling wave of the first kind (see, for example, [5]). The remaining constants $U_{(2)}$ and $U_{(3)}$ are chosen such that a nonlinear eigenvalue problem is satisfied. Accordingly, these phase velocities are dependent on the detailed structure of the solution which classifies them as travelling waves of the second kind (see, for example, [5]). Knowledge of the spectrum of this eigenvalue problem is essential in order to determine the travelling waves with more than one phase.

3.2 Solvability conditions

At next order, we have

$$L\boldsymbol{z} = \begin{pmatrix} \Delta u_0 + f(y) \\ \Delta v_0 \\ 0 \end{pmatrix}, \tag{3.3}$$

where

$$L = \begin{pmatrix} \bar{L} + \sum_{j=1}^{N} k \frac{\partial u_0}{\partial \theta_{(j)}} & \frac{\partial u_0}{\partial y} & \sum_{j=1}^{N} k \frac{\partial}{\partial \theta_{(j)}} \\ \sum_{j=1}^{N} k \frac{\partial v_0}{\partial \theta_{(j)}} & \bar{L} + \frac{\partial v_0}{\partial y} & \frac{\partial}{\partial y} \\ \sum_{j=1}^{N} k \frac{\partial}{\partial \theta_{(j)}} & \frac{\partial}{\partial y} & 0 \end{pmatrix}, \qquad \boldsymbol{z} = \begin{pmatrix} u_1 \\ v_1 \\ p_1 \end{pmatrix},$$

$$\Delta = \left(\sum_{j=1}^{N} k \frac{\partial}{\partial \theta_{(j)}} \right)^2 + \frac{\partial^2}{\partial y^2},$$

with the periodic boundary conditions

$$
\begin{aligned}
[u_1, v_1, p_1](0, \theta_{(2)}, \ldots, \theta_{(N)}, y) &= [u_1, v_1, p_1](2\pi, \theta_{(2)}, \ldots, \theta_{(N)}, y), \\
[u_1, v_1, p_1](\theta_{(1)}, 0, \ldots, \theta_{(N)}, y) &= [u_1, v_1, p_1](\theta_{(1)}, P_{(2)}, \ldots, \theta_{(N)}, y), \\
&\vdots \\
[u_1, v_1, p_1](\theta_{(1)}, \theta_{(2)}, \ldots, 0, y) &= [u_1, v_1, p_1](\theta_{(1)}, \theta_{(2)}, \ldots, P_{(N)}, y), \\
[u_1, v_1, p_1](\theta_{(1)}, \theta_{(2)}, \ldots, \theta_{(N)}, 0) &= [u_1, v_1, p_1](\theta_{(1)}, \theta_{(2)}, \ldots, \theta_{(N)}, 2\pi).
\end{aligned}
\tag{3.4}
$$

The right-hand side of (3.3) contains terms which, if not removed, would prevent the first correction (3.3)-(3.4) from having a solution. In this subsection, these terms are eliminated. Equation (3.3) is linear and thus the Fredholm alternative may be applied. The kernel of the adjoint problem corresponds to

$$L^* \boldsymbol{r} = 0 \tag{3.5}$$

in which

$$
L^* = \begin{pmatrix}
-\bar{L} + \sum_{j=1}^{N} k \dfrac{\partial u_0}{\partial \theta_{(j)}} & \sum_{j=1}^{N} k \dfrac{\partial v_0}{\partial \theta_{(j)}} & -\sum_{j=1}^{N} k \dfrac{\partial}{\partial \theta_{(j)}} \\
\dfrac{\partial u_0}{\partial y} & -\bar{L} + \dfrac{\partial v_0}{\partial y} & -\dfrac{\partial}{\partial y} \\
-\sum_{j=1}^{N} k \dfrac{\partial}{\partial \theta_{(j)}} & -\dfrac{\partial}{\partial y} & 0
\end{pmatrix}, \qquad \boldsymbol{r} = \begin{pmatrix} a \\ b \\ c \end{pmatrix},
$$

with the periodic boundary conditions

$$
\begin{aligned}
[a, b, c](0, \theta_{(2)}, \ldots, \theta_{(N)}, y) &= [a, b, c](2\pi, \theta_{(2)}, \ldots, \theta_{(N)}, y), \\
[a, b, c](\theta_{(1)}, 0, \ldots, \theta_{(N)}, y) &= [a, b, c](\theta_{(1)}, P_{(2)}, \ldots, \theta_{(N)}, y), \\
&\vdots \\
[a, b, c](\theta_{(1)}, \theta_{(2)}, \ldots, 0, y) &= [a, b, c](\theta_{(1)}, \theta_{(2)}, \ldots, P_{(N)}, y), \\
[a, b, c](\theta_{(1)}, \theta_{(2)}, \ldots, \theta_{(N)}, 0) &= [a, b, c](\theta_{(1)}, \theta_{(2)}, \ldots, \theta_{(N)}, 2\pi).
\end{aligned}
\tag{3.6}
$$

We will also require the definition

$$\langle \ \cdot \ \rangle_T = \frac{1}{\Omega} \int_{y=0}^{2\pi} \int_{\theta_{(N)}=0}^{P_{(N)}} \cdots \int_{\theta_{(2)}=0}^{P_{(2)}} \int_{\theta_{(1)}=0}^{2\pi} \cdot \ \mathrm{d}\theta_{(1)} \mathrm{d}\theta_{(2)} \ldots \mathrm{d}\theta_{(N)} \mathrm{d}y,$$

where

$$\Omega = (2\pi)^2 \prod_{j=2}^{N} P_{(j)}.$$

It follows from the Fredholm alternative that if $\boldsymbol{r}$ is in the kernel of the adjoint problem (3.5)-(3.6), then our linear problem for the first correction (3.3)-(3.4) can only have a solution if

$$\langle a \left[\Delta u_0 + f \right] + b \Delta v_0 \rangle_T = 0 \tag{3.7}$$

for any $\boldsymbol{r}$. Five linearly independent solutions of the adjoint problem (3.5)-(3.6) have been determined in [34, 39]:

$$\boldsymbol{r}_1 = (0,0,1)^T, \quad \boldsymbol{r}_2 = (1,0,u_0)^T, \quad \boldsymbol{r}_3 = (0,1,v_0)^T, \quad \boldsymbol{r}_4 = (u_0, v_0, p_0 + E_0)^T,$$

$$\boldsymbol{r}_5 = \left(\frac{\partial}{\partial y}(\omega_0^{m-1}), -\sum_{j=1}^{N} k \frac{\partial}{\partial \theta_{(j)}}(\omega_0^{m-1}), -\frac{(m-1)}{m}\omega_0^m \right)^T,$$

for $m \in \mathbb{N}$ and $m > 1$. The first three solutions are trivial solvability conditions owing to the periodicity. The solutions $\boldsymbol{r}_5$ correspond to a basis of the vector space of polynomials over the field of real numbers [39]. As the leading-order problem has shift-and-reflect symmetry (see Table 1), odd values of m in the fifth solvability condition also produce trivial equations [39]. We now consider the non-trivial solvability conditions. (i) If we substitute the fourth vector $\boldsymbol{r}_4$ into (3.7) and integrate by parts, then we obtain the kinetic energy solvability condition

$$\left\langle \left(\sum_{j=1}^{N} k \frac{\partial u_0}{\partial \theta_{(j)}} \right)^2 + \left(\frac{\partial u_0}{\partial y} \right)^2 + \left(\sum_{j=1}^{N} k \frac{\partial v_0}{\partial \theta_{(j)}} \right)^2 + \left(\frac{\partial v_0}{\partial y} \right)^2 - u_0 f \right\rangle_T = 0. \tag{3.8}$$

(ii) If we substitute the fifth vector $\boldsymbol{r}_5$ into (3.7) and again employ integration by parts, then we have the vorticity solvability conditions

$$\left\langle (m-1)\omega_0^{m-2} \left[\left(\sum_{j=1}^{N} k \frac{\partial \omega_0}{\partial \theta_{(j)}} \right)^2 + \left(\frac{\partial \omega_0}{\partial y} \right)^2 \right] + \omega_0^{m-1} \frac{\mathrm{d}f}{\mathrm{d}y} \right\rangle_T = 0, \tag{3.9}$$

for $m = 2, 4, 6, \ldots$.

These solvability conditions are necessary to define the manifold in phase space and control the amplitude of the flow. They would also be sufficient provided we have found all of the linearly independent solutions of the adjoint problem (3.5)-(3.6). Evidence that our solvability conditions are sufficient for the single-phased travelling wave is presented in Section 5. Provided we assume that the solvability conditions correspond to reformulations of (2.1)-(2.2), then this evidence also implies sufficiency for the quasi-periodic travelling waves (see the discussion in [34]).

The assumption that the solvability conditions of the Navier–Stokes equations correspond to reformulations of (2.1)-(2.2) should be viewed in the context of the literature. We consider three nonlinear differential equations in which the first correction is not self-adjoint: KdV [33], the Rayleigh–Plesset equation [37] and the single-mode rate equations [36]. In all three cases, the null space of the adjoint equation may be entirely determined and the solvability conditions all correspond to reformulations of the original equations. Hence, our assumption that the solvability conditions correspond to reformulations of (2.1)-(2.2) is consistent with all of the problems which are not self-adjoint in the literature.

Ablowitz and Benney [1] studied the nonlinear Klein–Gordon equation. For this equation, the first correction is self-adjoint, so the first correction and its adjoint have identical null spaces. The null spaces contain first derivatives of the leading-order solution with respect to each phase; that is, the number of solvability conditions increases as the number of phases increases. The first derivatives of the leading-order solution with respect to each phase are also in the null space of the first correction (3.3)-(3.4); however, our first correction is not self-adjoint and therefore these derivatives are not in the null space of the adjoint problem (3.5)-(3.6).

The vorticity solvability conditions (3.9) present a significant challenge for numerical methods. If $m \gg 1$ and $N = 1$, then double integrals of Laplace type need to be evaluated. If $m \gg 1$ and $N = 2$, then triple integrals of Laplace type are required. These integrals limit the numerical results in Sections 5 and 6.

4 Quasi-periodic standing wave

The asymptotic analysis of the family of quasi-periodic standing wave is an adaptation of the analysis of the family of multi-phased travelling wave in Section 3. In the interest of brevity, we only outline the result.

4.1 Leading-order problem

We adopt N fast time scales $T_{(j)}$ with

$$\frac{\mathrm{d}T_{(j)}}{\mathrm{d}t} = \Omega_{(j)},$$

where the frequencies $\Omega_{(j)}$ need to be chosen so that the period of oscillation is a constant on the $T_{(j)}$ scale and $N \in \{1, 2, 3\}$. We introduce expansions of the form

$$\begin{aligned}
u &\sim u_0(x, y, T_{(1)}, T_{(2)}, \ldots, T_{(N)}) + \epsilon u_1(x, y, T_{(1)}, T_{(2)}, \ldots, T_{(N)}),\\
v &\sim v_0(x, y, T_{(1)}, T_{(2)}, \ldots, T_{(N)}) + \epsilon v_1(x, y, T_{(1)}, T_{(2)}, \ldots, T_{(N)}),\\
p &\sim p_0(x, y, T_{(1)}, T_{(2)}, \ldots, T_{(N)}) + \epsilon p_1(x, y, T_{(1)}, T_{(2)}, \ldots, T_{(N)}),\\
\omega &\sim \omega_0(x, y, T_{(1)}, T_{(2)}, \ldots, T_{(N)}) + \epsilon \omega_1(x, y, T_{(1)}, T_{(2)}, \ldots, T_{(N)}),
\end{aligned}$$

as $\epsilon \to 0$. At leading order, we obtain

$$\hat{L}u_0 + \frac{\partial p_0}{\partial x} = 0, \qquad \hat{L}v_0 + \frac{\partial p_0}{\partial y} = 0, \qquad \frac{\partial u_0}{\partial x} + \frac{\partial v_0}{\partial y} = 0, \tag{4.1}$$

with the differential operator

$$\hat{L} = \sum_{j=1}^{N} \Omega_{(j)} \frac{\partial}{\partial T_{(j)}} + u_0 \frac{\partial}{\partial x} + v_0 \frac{\partial}{\partial y},$$

the periodic boundary conditions

$$\begin{aligned}
{}[u_0, v_0, p_0](0, y, T_{(1)}, \ldots, T_{(N)}) &= [u_0, v_0, p_0](2\pi/k, y, T_{(1)}, \ldots, T_{(N)}),\\
{}[u_0, v_0, p_0](x, 0, T_{(1)}, \ldots, T_{(N)}) &= [u_0, v_0, p_0](x, 2\pi, T_{(1)}, \ldots, T_{(N)}),\\
{}[u_0, v_0, p_0](x, y, T_{(1)}, \ldots, T_{(N)}) &= [u_0, v_0, p_0](x, y, T_{(1)} - n\hat{P}_{(1)}, \ldots, T_{(N)}),\\
&\ \ \vdots\\
{}[u_0, v_0, p_0](x, y, T_{(1)}, \ldots, T_{(N)}) &= [u_0, v_0, p_0](x, y, T_{(1)}, \ldots, T_{(N)} - n\hat{P}_{(N)}),
\end{aligned} \tag{4.2}$$

n is an integer and $\hat{P}_{(j)}$ are constant periods. As in Section 3, quasi-periodicity requires that none of $\hat{P}_{(1)}/\Omega_{(1)}$, $\hat{P}_{(2)}/\Omega_{(2)}$ and $\hat{P}_{(3)}/\Omega_{(3)}$ are rational multiples of another. The constants $\Omega_{(j)}$ with $j \in \{1, 2, 3\}$ are chosen such that the periodicity conditions (4.2) are satisfied on the $T_{(j)}$ scale.

4.2 Solvability conditions

The two solvability conditions are

$$\left\langle \left(\frac{\partial u_0}{\partial x}\right)^2 + \left(\frac{\partial u_0}{\partial y}\right)^2 + \left(\frac{\partial v_0}{\partial x}\right)^2 + \left(\frac{\partial v_0}{\partial y}\right)^2 - u_0 f \right\rangle_S = 0, \tag{4.3}$$

$$\left\langle (m-1)\omega_0^{m-2} \left[\left(\frac{\partial \omega_0}{\partial x}\right)^2 + \left(\frac{\partial \omega_0}{\partial y}\right)^2\right] + \omega_0^{m-1}\frac{\mathrm{d}f}{\mathrm{d}y} \right\rangle_S = 0, \tag{4.4}$$

for $m \in \mathbb{N}$ and $m > 1$ in which

$$\langle\ \boldsymbol{\cdot}\ \rangle_S = \frac{1}{\Omega}\int_{T_{(N)}=0}^{\hat{P}_{(N)}} \cdots \int_{T_{(2)}=0}^{\hat{P}_{(2)}} \int_{T_{(1)}=0}^{\hat{P}_{(1)}} \int_{y=0}^{2\pi} \int_{x=0}^{2\pi/k} \boldsymbol{\cdot}\ \mathrm{d}x\mathrm{d}y\mathrm{d}T_{(1)}\mathrm{d}T_{(2)}\ldots\mathrm{d}T_{(N)},$$

where

$$\Omega = \frac{(2\pi)^2}{k}\prod_{j=1}^{N}\hat{P}_{(j)}.$$

We note that symmetry conditions, such as the shift-and-rotate symmetry, would make (4.4) degenerate for odd values of m (see Table 1). The solvability conditions (4.4) for even positive values of m are necessary to define the manifold for the quasi-periodic standing waves. The kinetic energy solvability condition (4.3) is also necessary if the problem for the first correction is to have a solution.

As in Section 3, the vorticity solvability conditions (4.4) present a significant challenge for numerical methods. For example, if $m \gg 1$ and $N = 1$ for a periodic standing wave, then triple integrals of Laplace type are required.

5 Single-phased travelling wave

5.1 Introduction

This simpler case with a single phase is used to illustrate the asymptotic structure of one of Kolmogorov's attractors analysed in Section 3 and the role played by symmetry. The single-phased travelling wave corresponds to a relative equilibrium (steady state in a moving frame). Numerical simulations indicate that single-phased waves travelling in the positive x-direction dynamically develop shift-and-reflect symmetry which is imposed in the form (see Table 1)

$$[u, v](x, \pi + y, t) = [u, -v]\left(x + \frac{\pi}{k}, \pi - y, t\right).$$

Figure 2(a) shows a snapshot of a travelling wave with $R = 15$, $k = 1$ and $K = 2$ which exhibits this symmetry. The numerical method described in [38] has been employed on a

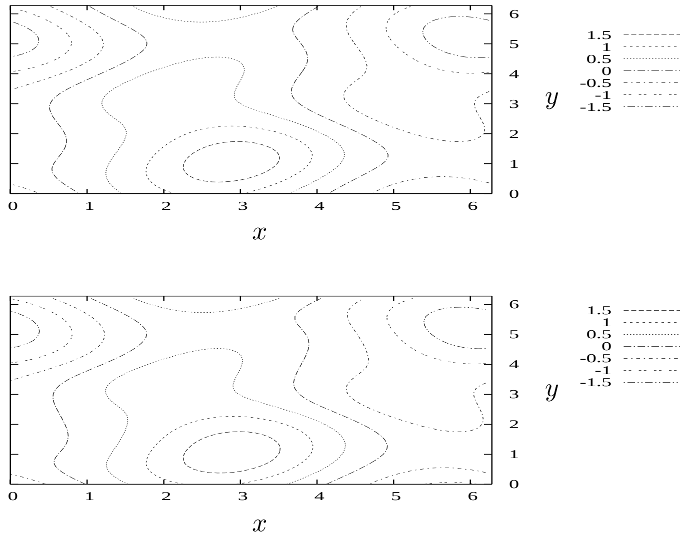

(b)

(a)

Figure 2. Comparison of the streamlines for a single-phased travelling wave with Reynolds number $R = 15$, aspect ratio $k = 1$ and forcing wavenumber $K = 2$ plotted in a coordinate system moving with the phase velocity $U_{(1)} = 1.55 \times 10^{-2}$: (a) direct numerical simulation of the Navier–Stokes equations (2.1)-(2.3); and (b) asymptotic analysis of the Navier–Stokes equations in Sections 3 and 5.

80×80 mesh. A second single-phased wave travelling in the positive x-direction is found by the transformation $y \to y + \pi$ as described in [2]. The corresponding waves in the negative x-direction are generated by the transformation $(x, y, u, v) \to (-x, -y + \pi/2, -u, -v)$. The set of solutions connected by these two group operations forms a group orbit; only one member of this group needs to be calculated.

5.2 Analysis

In this subsection, the general analysis of Section 3 is applied to the relative equilibrium. We have a single phase ($\theta_{(1)} = \theta$). The periodic boundary conditions (3.2) are supplemented by the shift-and-reflect symmetry condition

$$[u_0, v_0](\theta, \pi + y) = [u_0, -v_0](\theta + \pi, \pi - y).$$

We define a stream function $\psi(\theta, y)$ by the equations

$$u_0 = U_{(1)} + \frac{\partial \psi}{\partial y}, \qquad v_0 = -k \frac{\partial \psi}{\partial \theta}.$$

The vorticity equation may be rewritten as

$$\frac{\partial \psi}{\partial y} \frac{\partial \omega_0}{\partial \theta} = \frac{\partial \psi}{\partial \theta} \frac{\partial \omega_0}{\partial y} \tag{5.1}$$

in which

$$\omega_0 = -k^2 \frac{\partial^2 \psi}{\partial \theta^2} - \frac{\partial^2 \psi}{\partial y^2}, \tag{5.2}$$

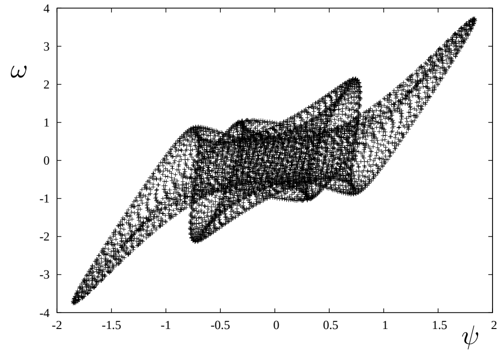

Figure 3. Scatter plot of the stream function ψ versus the vorticity ω with Reynolds number $R = 15$, aspect ratio $k = 1$ and forcing wavenumber $K = 2$ for the single-phased travelling wave in Figure 2(a). The absence of a first integral of (5.1) in the form $\omega_0 = V(\psi)$ is demonstrated.

with the periodic boundary conditions

$$\psi(0, y) = \psi(2\pi, y), \qquad \psi(\theta, 0) = \psi(\theta, 2\pi) \tag{5.3}$$

and shift-and-reflect symmetry condition

$$\psi(\theta, \pi + y) = -\psi(\theta + \pi, \pi - y). \tag{5.4}$$

Before we proceed with the analysis of (5.1)-(5.4), two points are noteworthy: (i) The phase velocity $U_{(1)}$ has been eliminated from (5.1)-(5.4). The transient problem must be considered to determine its value. (ii) The absence of a first integral of (5.1) in the form $\omega_0 = V(\psi)$ is shown in Figure 3. Therefore there is no maximum-entropy configuration [14, 22, 23] for this travelling wave in contrast to two-dimensional plane Poiseuille flow [39].

The periodicity in θ allows us to express the stream function as a complex Fourier series

$$\psi = \sum_{n=-\infty}^{\infty} c_n(y) e^{in\theta},$$

where $c_{-n} = c_n^*$ and * denotes complex conjugate. We note that only a finite number of the c_n are non-zero because viscous effects would reappear at leading order when $n = \mathcal{O}(R^{1/2})$. Using (5.1)-(5.2), we obtain the system of ordinary differential equations in y

$$\sum_{j=-\infty}^{\infty} j \frac{\mathrm{d}c_{n-j}}{\mathrm{d}y} \left[\frac{\mathrm{d}^2 c_j}{\mathrm{d}y^2} - k^2 j^2 c_j \right] = \sum_{j=-\infty}^{\infty} (n-j) c_{n-j} \left[\frac{\mathrm{d}^3 c_j}{\mathrm{d}y^3} - k^2 j^2 \frac{\mathrm{d}c_j}{\mathrm{d}y} \right] \tag{5.5}$$

for $n \in \mathbb{N}$. The periodic boundary conditions and the shift-and-reflect symmetry conditions become $c_n(0) = c_n(2\pi)$, $c_n(\pi - y) = -c_n(\pi + y)$ if n is even and $c_n(\pi - y) = c_n(\pi + y)$ if n is odd. The third-order ordinary differential equations (5.5) have only two boundary conditions for each $n \in \mathbb{N}$. One solvability condition (3.9) for $n = 0$ and two solvability conditions (3.9) for each value of $n \neq 0$ are required to ensure a unique solution is obtained. The solution determined in this manner must also satisfy the kinetic energy solvability condition (3.8).

5.3 Numerical method

The numerical method is based on an approximate solution of the leading-order problem in the form of a truncated double Fourier series. The periodicity boundary conditions (5.3) and shift-and-reflect symmetry condition (5.4) will be exactly satisfied by this series, but equations (3.8), (3.9) and (5.1) will not. The truncated double Fourier series is

$$\psi = \sum_{n=0}^{n_{even}} \sum_{s=1}^{s_{odd}} a_{ns} \sin(sy) \cos(2n\theta) + \sum_{n=1}^{n_{even}} \sum_{s=1}^{s_{odd}} b_{ns} \sin(sy) \sin(2n\theta)$$
$$+ \sum_{n=0}^{n_{odd}} \sum_{s=0}^{s_{even}} \cos(sy) \left[c_{ns} \cos((2n+1)\theta) + d_{ns} \sin((2n+1)\theta)\right], \tag{5.6}$$

where the coefficients a_{ns}, b_{ns}, c_{ns} and d_{ns} parameterize an M-dimensional phase space in which

$$M = s_{odd}(2n_{even} + 1) + 2(s_{even} + 1)(n_{odd} + 1).$$

In order to determine these M unknowns, we require M equations. Using the orthogonality properties of circular functions, we require the following equations to hold in order to satisfy (5.1):

$$\int_{y=0}^{2\pi} \int_{\theta=0}^{2\pi} \left\{ \frac{\partial \psi}{\partial y} \frac{\partial \omega_0}{\partial \theta} - \frac{\partial \psi}{\partial \theta} \frac{\partial \omega_0}{\partial y} \right\} \sin(sy) \cos(2n\theta) \mathrm{d}\theta \mathrm{d}y = 0,$$

for $n = 0, \ldots, n_{even}$ and $s = 1, \ldots, s_{odd} - 1$ and

$$\int_{y=0}^{2\pi} \int_{\theta=0}^{2\pi} \left\{ \frac{\partial \psi}{\partial y} \frac{\partial \omega_0}{\partial \theta} - \frac{\partial \psi}{\partial \theta} \frac{\partial \omega_0}{\partial y} \right\} \sin(sy) \sin(2n\theta) \mathrm{d}\theta \mathrm{d}y = 0,$$

for $n = 1, \ldots, n_{even}$ and $s = 1, \ldots, s_{odd} - 1$. Similar algebraic equations are formulated for the third sum in (5.6). In total, we have r equations of this form in which

$$r = (s_{odd} - 1)(2n_{even} + 1) + 2s_{even}(n_{odd} + 1).$$

An r-dimensional manifold is now constructed using the $M - r$ solvability conditions (3.9). We define a vector function on the phase space as follows

$$\mathbf{\Phi} = (\Phi^1, \Phi^2, \ldots, \Phi^{M-r})$$

in which Φ^1 is the left-hand side of (3.9) with $m = 2$, Φ^2 is the left-hand side of (3.9) with $m = 4$, …, Φ^{M-r} is the left-hand side of (3.9) with $m = 2(M - r)$. The $M - r$ equations given by $\mathbf{\Phi} = \mathbf{0}$ complete the system of M equations. We note that the equation $\mathbf{\Phi} = \mathbf{0}$ describes an r-dimensional manifold in the M-dimensional phase space.

The double integrals above are performed using the NAG routine D01EAF which employs an adaptive subdivision strategy and the resulting system of nonlinear algebraic equations is solved via the modified Powell hybrid method in NAG routine C05NBF.

5.4 Numerical results

We now seek a comparison with the direct numerical solution shown in Figure 2(a) for the single-phased travelling wave at $R = 15$, $k = 1$ and $K = 2$ (see Figure 1). In order to gain suitable resolution in (5.6), we adopt $n_{even} = 2$, $n_{odd} = 1$, $s_{even} = 4$ and $s_{odd} = 4$ which corresponds to a truncation of the order of $R^{1/2}$, a 31-dimensional manifold and a 40-dimensional phase space. This resolution may be evaluated by considering the numerical error in the kinetic energy solvability equation (3.8), which is 2.6×10^{-2} for this truncation. The prediction of the travelling wave is shown in Figure 2(b). The stream function has been plotted with the same contours as in Figure 2(a) in order to facilitate comparison. The agreement between Figures 2(a) and 2(b) is remarkable given that the next term in the expansion is $\mathcal{O}(1/R)$. In fact, the errors appear at $\mathcal{O}(1/R^2)$.

6 Two-phased travelling wave

6.1 Introduction

We are now in a position to investigate how the asymptotic structure of the single-phased travelling wave in Section 5 is transformed by the Hopf bifurcation at a Reynolds number of approximately 22 (see Figure 1). The two-phased travelling wave corresponds to a relative periodic orbit (a flow which is periodic in a moving frame). In the Cartesian coordinate system, a relative periodic orbit is a time-dependent velocity field which satisfies

$$\boldsymbol{q}(x, y, t + T) = \boldsymbol{q}(x + \Delta x, y, t), \tag{6.1}$$

for constant period T and constant spatial translation Δx. Furthermore numerical simulations show that a two-phased wave travelling in the positive x-direction will have the following spatio-temporal symmetry (see Table 1)

$$[u, v](x, \pi + y, t) = [u, -v]\left(x + \frac{\pi}{k}, \pi - y, t + \frac{T}{2}\right). \tag{6.2}$$

Three other two-phased travelling waves may be generated by the same transformations as described for single-phased travelling waves in Section 5.1 and in [2].

6.2 Analysis

The general analysis of Section 3 is now applied to the relative periodic orbit with $N = 2$. We have the shift-and-reflect symmetry condition in the second phase

$$[u_0, v_0](\theta_{(1)}, \theta_{(2)}, \pi + y) = [u_0, -v_0]\left(\theta_{(1)}, \theta_{(2)} + \frac{P_{(2)}}{2}, \pi - y\right),$$

in which the period $P_{(2)}$ is specified to be

$$P_{(2)} = 2\pi\left(1 - \frac{U_{(2)}}{U_{(1)}}\right). \tag{6.3}$$

The restriction (6.3) on the period follows from (6.2); it is also consistent with (6.1). Furthermore, quasi-periodicity requires that $U_{(2)}/U_{(1)}$ is not a rational number. We note that it would be incorrect to specify $P_{(2)}$ to be an arbitrary constant in this case even though it was permitted to specify the period in previous studies [32, 35]. We now redefine the stream function $\psi(\theta_{(1)}, \theta_{(2)}, y)$ by the equations

$$u_0 = U_{(1)} + \frac{\partial\psi}{\partial y}, \qquad v_0 = -k\left(\frac{\partial\psi}{\partial\theta_{(1)}} + \frac{\partial\psi}{\partial\theta_{(2)}}\right).$$

The nonlinear eigenvalue problem, which determines the two-phased travelling wave, is given by

$$\frac{\partial\psi}{\partial y}\left(\frac{\partial\omega_0}{\partial\theta_{(1)}} + \frac{\partial\omega_0}{\partial\theta_{(2)}}\right) + \lambda\frac{\partial\omega_0}{\partial\theta_{(2)}} = \frac{\partial\omega_0}{\partial y}\left(\frac{\partial\psi}{\partial\theta_{(1)}} + \frac{\partial\psi}{\partial\theta_{(2)}}\right), \tag{6.4}$$

in which the eigenvalue $\lambda = U_{(1)} - U_{(2)}$ and

$$\omega_0 = -k^2\left(\frac{\partial^2\psi}{\partial\theta_{(1)}^2} + 2\frac{\partial^2\psi}{\partial\theta_{(1)}\partial\theta_{(2)}} + \frac{\partial^2\psi}{\partial\theta_{(2)}^2}\right) - \frac{\partial^2\psi}{\partial y^2}, \tag{6.5}$$

with the periodic boundary conditions

$$\psi(0, \theta_{(2)}, y) = \psi(2\pi, \theta_{(2)}, y), \tag{6.6 a}$$

$$\psi(\theta_{(1)}, 0, y) = \psi(\theta_{(1)}, P_{(2)}, y), \tag{6.6 b}$$

$$\psi(\theta_{(1)}, \theta_{(2)}, 0) = \psi(\theta_{(1)}, \theta_{(2)}, 2\pi), \tag{6.6 c}$$

shift-and-reflect symmetry condition in the second phase

$$\psi(\theta_{(1)}, \theta_{(2)}, \pi + y) = -\psi\left(\theta_{(1)}, \theta_{(2)} + \frac{P_{(2)}}{2}, \pi - y\right) \tag{6.7}$$

and solvability conditions (3.9).

We now proceed to the analysis of the nonlinear eigenvalue problem. The periodicity in $\theta_{(1)}$ and $\theta_{(2)}$ allows us to introduce the complex Fourier series

$$\psi = \sum_{l=-\infty}^{\infty}\sum_{n=-\infty}^{\infty} c_{l,n}(y)e^{i\phi_{l,n}},$$

where $\phi_{l,n} = l\theta_{(1)} + 2\pi n\theta_{(2)}/P_{(2)}$ and $c_{-l,-n} = c^*_{l,n}$. We note that only a finite number of the $c_{l,n}$ are non-zero because viscous effects would appear at leading order when $l = \mathcal{O}(R^{1/2})$ or $n = \mathcal{O}(R^{1/2})$. Using (6.4)-(6.5), we have for $l \in \mathbb{N}$ and $n \in \mathbb{N}$

$$\lambda\frac{2\pi n}{P_{(2)}}\left(\frac{\mathrm{d}^2 c_{l,n}}{\mathrm{d}y^2} - k^2A_{l,n}^2c_{l,n}\right) + \sum_{r=-\infty}^{\infty}\sum_{s=-\infty}^{\infty} A_{r,s}\left(\frac{\mathrm{d}^2c_{r,s}}{\mathrm{d}y^2} - k^2A_{r,s}^2c_{r,s}\right)\frac{\mathrm{d}c_{l-r,n-s}}{\mathrm{d}y}$$

$$= \sum_{r=-\infty}^{\infty}\sum_{s=-\infty}^{\infty} A_{l-r,n-s}\left(\frac{\mathrm{d}^3c_{r,s}}{\mathrm{d}y^3} - k^2A_{r,s}^2\frac{\mathrm{d}c_{r,s}}{\mathrm{d}y}\right)c_{l-r,n-s},$$

in which $A_{l,n} = l + 2\pi n/P_{(2)}$. The boundary conditions become $c_{l,n}(0) = c_{l,n}(2\pi)$, $c_{l,n}(\pi + y) = -c_{l,n}(\pi - y)$ if n is even and $c_{l,n}(\pi + y) = c_{l,n}(\pi - y)$ if n is odd. To complete the nonlinear eigenvalue problem, we have one solvability condition (3.9) for $l = n = 0$ and two solvability conditions (3.9) for every other combination of l and n. Any such solution must also satisfy the kinetic energy solvability condition (3.8). A numerical solution

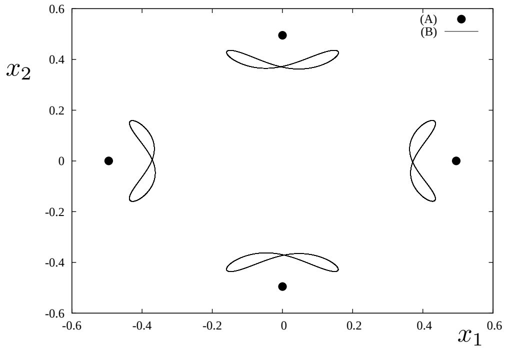

Figure 4. Projections of (A) four unstable single-phased travelling waves and (B) a four stable two-phased travelling waves onto the (x_1, x_2) plane. The parameters are Reynolds number $R = 25$, aspect ratio $k = 1$ and forcing wavenumber $K = 2$ and the numerical simulation takes place on a 80×80 mesh. Single-phased and two-phased waves are studied in Sections 3 and 5 and Sections 3 and 6, respectively.

would require the evaluation of triple integrals of Laplace type in (3.9) which is beyond the scope of this article.

6.3 Direct numerical simulation

A comparison of the stable two-phased travelling waves and unstable single-phased travelling waves is now sought. We adopt the parameters $R = 25$, $k = 1$ and $K = 2$. A direct numerical simulation is then undertaken on a 80×80 mesh. The solution approaches a stable two-phased travelling wave propagating in the positive x-direction. In a similar manner to [2], we define

$$x_1 = \frac{1}{2\pi^2} \int_{y=0}^{2\pi} \int_{x=0}^{2\pi} u \sin(y)\, \mathrm{d}x\, \mathrm{d}y, \qquad x_2 = \frac{1}{2\pi^2} \int_{y=0}^{2\pi} \int_{x=0}^{2\pi} u \cos(y)\, \mathrm{d}x\, \mathrm{d}y.$$

Figure 4 shows a two-dimensional projection of phase space in which this two-phased wave is the figure-of-eight shape in $x_2 > 0$. A second stable two-phased wave travelling in the positive x-direction is found by the transformation $y \to y + \pi$ (shown in $x_2 < 0$ in Figure 4). The corresponding waves in the negative x-direction are generated by the transformation $(x, y, u, v) \to (-x, -y + \pi/2, -u, -v)$, these being shown in $x_1 > 0$ and $x_1 < 0$ in Figure 4.

For comparison, unstable single-phased travelling waves are evaluated at the same Reynolds number using the asymptotic approach in Section 5. We require $n_{even} = 2$, $n_{odd} = 2$, $s_{even} = 5$ and $s_{odd} = 5$ in (5.6) which corresponds to a truncation of the double Fourier series of the order of $R^{1/2}$, a 50-dimensional manifold and a 61-dimensional phase space. The resolution may be assessed by considering the numerical error in the kinetic energy solvability equation (3.8), which is 3.6×10^{-2} for this truncation. The other three travelling waves are generated by using the symmetries. These four unstable non-wandering sets are also shown in Figure 4.

The stable two-phased travelling waves and unstable single-phased travelling waves in

Figure 4 represent two solution branches. The two-phased waves originated at a supercritical Hopf bifurcation from the branch of single-phased waves and, at this bifurcation, the single-phased waves have lost their stability ($R = 22$ as shown in Figure 1). The two solution branches may be seen to have moved apart as the Reynolds number increased from $R = 22$ to $R = 25$. If we adopt $\alpha = \sqrt{x_1^2 + x_2^2}$ as a measure of (local) amplitude, then the amplitude of the single-phased wave is always greater than the amplitude of the two-phased wave. Amplitudes are governed by the solvability conditions (3.9) for both single-phased and two-phased waves.

7 Chaotic/turbulent attractor

Ladyzhenskaya [17] established the existence of the chaotic or turbulent attractor for the two-dimensional Navier–Stokes equations. The asymptotic analysis in this article does not apply directly to the chaotic or turbulent attractor. Our indirect approach exploits the well-known fact that the invariant manifold of these attractors must contain any unstable non-wandering sets. For sufficiently high Reynolds number, after the bifurcation to chaotic flow, these unstable non-wandering sets not only comprise the families of travelling and standing waves studied in Sections 3 and 4, but also any other unstable travelling and standing waves in phase space. Provided the following conditions hold

(i) the leading-order problem is governed by the Euler equations; and

(ii) an appropriate symmetry exists to eliminate the trivial solvability conditions;

then the equations (3.8)-(3.9) and (4.3)-(4.4) are necessary conditions to describe these travelling and standing waves. Therefore, the invariant manifold of the chaotic or turbulent attractor must encompass the manifolds given by (3.8)-(3.9) and (4.3)-(4.4). As these non-wandering sets in the invariant manifold are unstable, it should be borne in mind that the manifolds (3.8)-(3.9) and (4.3)-(4.4) may have more than three fundamental frequencies; that is, $N > 3$ in Sections 3 and 4.

Based on our asymptotic analysis, we conjecture that the invariant manifold for the chaotic or turbulent attractor is defined by

$$\lim_{\tau\to\infty} I_1(\tau) = \lim_{\tau\to\infty} I_2(\tau; m) = 0, \tag{7.1}$$

in which

$$I_1(\tau) \equiv \left\langle \left(\frac{\partial u}{\partial x}\right)^2 + \left(\frac{\partial u}{\partial y}\right)^2 + \left(\frac{\partial v}{\partial x}\right)^2 + \left(\frac{\partial v}{\partial y}\right)^2 - uf \right\rangle,$$

$$I_2(\tau; m) \equiv \left\langle (m-1)\omega^{m-2}\left[\left(\frac{\partial \omega}{\partial x}\right)^2 + \left(\frac{\partial \omega}{\partial y}\right)^2\right] + \omega^{m-1}\frac{\mathrm{d}f}{\mathrm{d}y} \right\rangle$$

and

$$\langle\ \cdot\ \rangle = \frac{1}{\tau}\int_{t=0}^{\tau}\int_{y=0}^{2\pi}\int_{x=0}^{2\pi} \cdot \ \mathrm{d}x\mathrm{d}y\mathrm{d}t,$$

where $m = 2, 4, 6, \ldots, \kappa$. The upper bound κ arises from the finite number of degrees of freedom required to describe the attractor. In the case of the turbulent attractor, the number of degrees of freedom in a domain of size $(L^*/k) \times L^*$ may be assumed to be of the order of

$$\zeta = \frac{L^{*\,2}}{\lambda_K^2 k},$$

in which λ_K is Kraichnan's length. The upper bound κ is itself bounded above by ζ, but κ will be much less than ζ in practice.

The necessity of conditions (7.1) may be seen by considering the equations

$$\frac{\partial E}{\partial t} + \frac{\partial}{\partial x}(u[p+E]) + \frac{\partial}{\partial y}(v[p+E]) = \epsilon \left\{ \frac{\partial}{\partial x}\left(u\frac{\partial u}{\partial x} + v\frac{\partial v}{\partial x} \right) \right.$$
$$\left. + \frac{\partial}{\partial y}\left(u\frac{\partial u}{\partial y} + v\frac{\partial v}{\partial y} \right) - \left(\frac{\partial u}{\partial x}\right)^2 - \left(\frac{\partial u}{\partial y}\right)^2 - \left(\frac{\partial v}{\partial x}\right)^2 - \left(\frac{\partial v}{\partial y}\right)^2 + uf \right\}, \qquad (7.2)$$

$$\frac{\partial}{\partial t}(\omega^m) + \frac{\partial}{\partial x}(u\omega^m) + \frac{\partial}{\partial y}(v\omega^m) = \epsilon m \left\{ \frac{\partial}{\partial x}\left(\omega^{m-1}\frac{\partial \omega}{\partial x} \right) \right.$$
$$\left. + \frac{\partial}{\partial y}\left(\omega^{m-1}\frac{\partial \omega}{\partial y} \right) - (m-1)\omega^{m-2}\left[\left(\frac{\partial \omega}{\partial x}\right)^2 + \left(\frac{\partial \omega}{\partial y}\right)^2 \right] - \omega^{m-1}\frac{\mathrm{d}f}{\mathrm{d}y} \right\}. \qquad (7.3)$$

Using periodicity, we integrate (7.2)-(7.3) to obtain

$$\frac{1}{\tau}\int_{y=0}^{2\pi}\int_{x=0}^{2\pi} E(x,y,\tau) - E(x,y,0)\ \ \mathrm{d}x\mathrm{d}y = -\epsilon I_1(\tau), \qquad (7.4)$$

$$\frac{1}{\tau}\int_{y=0}^{2\pi}\int_{x=0}^{2\pi} \omega(x,y,\tau)^m - \omega(x,y,0)^m\ \ \mathrm{d}x\mathrm{d}y = -\epsilon m I_2(\tau;m). \qquad (7.5)$$

Provided the integrals on the left-hand side of (7.4)-(7.5) remain finite for large τ, the left-hand side tends to zero as τ tends to infinity and equations (7.1) are necessary conditions. Hence, the invariant manifold given by (7.1) bounds the chaotic or turbulent attractor in phase space.

8 Summary and conclusions

In this article, we have investigated the high-Reynolds-number asymptotic structure of the laminar attractors in a two-dimensional Kolmogorov flow. At leading order, the attractors under study are assumed to be governed by the Euler equations. In this case, we found no evidence for the existence of a first integral in the form of a maximum-entropy configuration. At the next order, solvability conditions suppressing secular terms have been determined. We found that these conditions correspond to a countably infinite number of vorticity equations and a single kinetic energy equation. In this case, a finite number of the vorticity solvability conditions determined a manifold. For each laminar attractor, the Euler equations had to be solved on this manifold, subject to the appropriate periodicity and symmetry conditions. Viscosity limited the dimension of phase space via the smallest scales and, in each case, the manifold was of almost the same dimension as its underlying phase space which made visualization difficult.

The analysis of single-phased and multi-phased travelling waves has revealed a novel mathematical structure. For the single-phased travelling wave, we showed that the phase velocity is determined by the integral conservation law for kinetic energy and is completely independent of the detailed structure of the solution. Thus, we have discovered a standard travelling wave of the first kind. For the multi-phased travelling wave, we found that the first phase velocity is still determined by the integral conservation law for kinetic energy and remains independent of the exact structure of the solution. However, in this case, the integral conservation law is insufficient for the evaluation of subsequent phase velocities. We demonstrated that these subsequent phase velocities can be determined as eigenvalues in the process of finding the shape and form of the solution. In summary, the first phase velocity corresponds to a travelling wave of the first kind, whereas the other phase velocities behave consistently with travelling waves of the second kind.

As demonstrated in the course of our analysis, the effects of viscosity can be used not only to evaluate the smallest scales, but also to determine the amplitude of the flow via the manifold. We show that the shape and form of the flow is governed entirely by the inertial effects at leading order. Furthermore, there are two clear indications that the viscous terms can be entirely eliminated at order $1/R$ by the solvability conditions: (i) the errors in the cross correlation in Table 1 of [38] are of the order of $1/R^2$; and (ii) the agreement between direct numerical simulation and asymptotic analysis in Figure 2 is also of the order of $1/R^2$.

The comparison of our analytical predictions for evaluating the stable single-phased travelling wave with the direct numerical simulation of the Navier–Stokes equations has been undertaken, the agreement being excellent. We drew two key conclusions from our comparison. Firstly, the solvability conditions are not only necessary, but also sufficient for the first correction to have a solution, provided we assume that the solvability conditions correspond to reformulations of (2.1)-(2.2). Secondly, the proposed asymptotic structure of the laminar attractors of the Navier–Stokes equations has been numerically validated. The first conclusion also served to confirm the sufficiency of the modulation equations in our previous analysis of two-dimensional plane Poiseuille flow [39].

We summarize our results on the invariant manifolds of laminar attractors. Our three assumptions are as follows:

(i) The leading-order problem is governed by the Euler equations.

(ii) An appropriate symmetry exists to eliminate the trivial solvability conditions.

(iii) The solvability conditions correspond to reformulations of (2.1)-(2.2).

Assumptions (i) and (ii) are required to show necessity. Furthermore, if we also have assumption (iii), then we may establish sufficiency. Given these three assumptions, the invariant manifolds of multi-phased travelling waves and quasi-periodic standing waves have been identified as (3.8)-(3.9) and (4.3)-(4.4), respectively. We note that these travelling waves and standing waves will not only comprise those involved in the transition process, but also any others of this kind in phase space.

For sufficiently high Reynolds number, after the bifurcation to chaotic flow, all of the multi-phased travelling waves and quasi-periodic standing waves become unstable non-wandering sets. Taking into account that the invariant manifold of the chaotic and turbulent attractor must contain these unstable non-wandering sets and based on our asymptotic analysis of the manifolds of these sets, necessary conditions have been identified to enable us to bound the invariant manifold of the chaotic and turbulent flow in phase space. These conditions constitute a finite number of vorticity conditions and a single kinetic energy condition. We observe that, for more general flows, there should also be a necessary condition for conservation of mass and two necessary conditions for conservation of momentum.

References

[1] Ablowitz, M. J., and Benney, D. J. The evolution of multi-phase modes for nonlinear dispersive waves. *Stud. Appl. Math. 49* (1970), 225–238.

[2] Armbruster, D., Nicolaenko, B., Smaoui, N., and Chossat, P. Symmetries and dynamics for 2-D Navier–Stokes flow. *Physica D 95* (1996), 81–93.

[3] Arnol'd, V. I. Kolmogorov's hydrodynamic attractors. *Proc. R. Soc. Lond. A 434* (1991), 19–22.

[4] Arnol'd, V. I., and Meshalkin, L. D. The seminar of A. N. Kolmogorov on selected topics in analysis (1958-59). *Usp. Mat. Nauk 15* (1960), 247–250.

[5] Barenblatt, G. I. *Scaling, self-similarity, and intermediate asymptotics.* Cambridge University Press, Cambridge, 1996.

[6] Bowles, R. I., Davies, C., and Smith, F. T. On the spiking stages in deep transition and unsteady separation. *J. Eng. Math 45* (2003), 227–245.

[7] Chapman, S. J. Subcritical transition in channel flows. *J. Fluid Mech. 451* (2002), 35–97.

[8] Craik, A. D. D. *Wave interactions and fluid flows.* Cambridge University Press, Cambridge, 1985.

[9] Deguchi, K., and Walton, A. G. A swirling spiral wave solution in pipe flow. *J. Fluid Mech. 737* (2013), R2.

[10] Farazmand, M. An adjoint-based approach for finding invariant solutions of Navier–Stokes equations. *J. Fluid Mech. 795* (2016), 278–312.

[11] Hall, P., and Smith, F. T. On strongly nonlinear vortex/wave interactions in boundary-layer transition. *J. Fluid Mech. 227* (1991), 641–666.

[12] Hiruta, Y., and Toh, S. Solitary solutions including spatially localized chaos and their interactions in two-dimensional Kolmogorov flow. *Phys. Rev. E 92* (2015), 063025.

[13] Hopf, E. A mathematical example displaying features of turbulence. *Comm. Pure Appl. Math. 1* (1948), 303–322.

[14] Joyce, G. R., and Montgomery, D. Negative temperature states for a two-dimensional guiding-center plasma. *J. Plasma Phys. 10* (1973), 107–121.

[15] Kim, S-C., and Okamoto, H. Unimodal patterns appearing in the Kolmogorov flows at large Reynolds numbers. *Nonlinearity 28* (2015), 3219–3242.

[16] Kuzmak, G. E. Asymptotic solutions of nonlinear second order differential equations with variable coefficients. *Prikl. Mat. Mekh. 23* (1959), 515–526. (In Russian) J. Appl. Math. Mech., 23 (1959), pp. 730-744.(In English).

[17] Ladyzhenskaya, O. A. A dynamical system generated by the navier–stokes equations. *Zap. Nauchn. Sem. Leningrad Otdel. Mat. Inst. Steklov (LOMI) 27* (1972), 91–115. (In Russian) J. Soviet Math., 3 (1975), pp. 458-479.(In English).

[18] Landau, L. D., and Lifshitz, E. M. *Fluid Mechanics.* Pergamon Press, Oxford, 1987.

[19] Lucas, D., and Kerswell, R. R. Recurrent flow analysis in spatiotemporally chaotic 2-dimensional Kolmogorov flow. *Phys. Fluids 27* (2015), 045106.

[20] Luke, J. C. A perturbation method for nonlinear dispersive wave problems. *Proc. Roy. Soc. Lond. A 292* (1966), 403–412.

[21] Meshalkin, L. D., and Ya. G. Sinai. Investigation of the stability of a stationary solution of a system of equations for the plane movement of an incompressible viscous liquid. *Prikl. Mat. Mekh. 25* (1961), 1140–1143. (In Russian) J. Appl. Math. Mech., 25 (1961), pp. 1700-1705.(In English).

[22] Montgomery, D., and Joyce, G. R. Statistical mechanics of "negative temperature" states. *Phys. Fluids 17* (1974), 1139–1145.

[23] Montgomery, D., Matthaeus, W. H., Stribling, W. T., Martinez, D., and Oughton, S. Relaxation in two dimensions and the "sinh-Poisson" equation. *Phys. Fluids A 4* (1992), 3–6.

[24] Newhouse, S. E., Ruelle, D., and Takens, F. Occurrence of strange axiom A attractors near quasi-periodic flows on T^m, $m \geqslant 3$. *Comm. Math. Phys. 64* (1978), 35–40.

[25] Okamoto, H., and Shoji, M. Bifurcation diagrams in Kolmogorov's problem of viscous incompressible fluid on 2-D flat tori. *Japan J. Indust. Appl. Math. 10* (1993), 191–218.

[26] Platt, N., Sirovich, L., and Fitzmaurice, N. An investigation of chaotic Kolmogorov flows. *Phys. Fluids A 3* (1991), 681–696.

[27] Ruelle, D., and Takens, F. On the nature of turbulence. *Comm. Math. Phys. 20* (1971), 167–192.

[28] She, Z. S. Large-scale dynamics and transition to turbulence in the two-dimensional Kolmogorov flow. In *Proceedings on Current Trends in Turbulence Research* (1988), H. Branover, M. Mond, and Y. Unger, Eds., vol. 117, AIAA, pp. 374–396.

[29] Smith, F. T., and Bodonyi, R. J. Amplitude-dependent neutral modes in the Hagen-Poiseuille flow through a circular pipe. *Proc. R. Soc. Lond. A 384* (1982), 463–489.

[30] Smith, F. T., and Burggraf, O. R. On the development of large-sized short-scaled disturbances in boundary layers. *Proc. R. Soc. Lond. A 399* (1985), 25–55.

[31] Smith, F. T., Doorly, D. J., and Rothmayer, A. P. On displacement-thickness, wall-layer and mid-flow scales in turbulent boundary layers, and slugs of vorticity in channel and pipe flows. *Proc. R. Soc. Lond. A 428* (1990), 255–281.

[32] Smith, W. R. On the sensitivity of strongly nonlinear autonomous oscillators and oscillatory waves to small perturbations. *IMA J. Appl. Math. 70* (2005), 359–385.

[33] Smith, W. R. Explicit modulation equations, Reynolds averaging and the closure problem for the Korteweg-deVries-Burgers equation. *IMA J. Appl. Math. 72* (2007), 163–179.

[34] Smith, W. R. Modulation equations and Reynolds averaging for finite-amplitude nonlinear waves in an incompressible fluid. *IMA J. Appl. Math. 72* (2007), 923–945.

[35] Smith, W. R. Modulation equations for strongly nonlinear oscillations of an incompressible viscous drop. *J. Fluid Mech. 654* (2010), 141–159.

[36] Smith, W. R., King, J. R., Tuck, B., and Orton, J. W. The single-mode rate equations for semiconductor lasers with thermal effects. *IMA J. Appl. Math. 63* (1999), 1–36.

[37] Smith, W. R., and Wang, Q. X. Viscous decay of nonlinear oscillations of a spherical bubble at large Reynolds number. In preparation.

[38] Smith, W. R., and Wissink, J. G. Parameterization of travelling waves in plane Poiseuille flow. *IMA J. Appl. Math. 79* (2014), 22–32.

[39] Smith, W. R., and Wissink, J. G. Travelling waves in two-dimensional plane Poiseuille flow. *SIAM J. Appl. Math. 75* (2015), 2147–2169.

[40] Tennekes, H., and Lumley, J. L. *A First Course in Turbulence.* MIT Press, London, 1972.

[41] Whitham, G. B. *Linear and Nonlinear Waves.* John Wiley & Sons, New York, 1974.